# Circumstellar Material Around Evolved Massive Stars

Nathan Smith[1,2]

[1] Steward Observatory, University of Arizona, 933 N. Cherry Ave., Tucson, AZ, 85721, USA
[2] Astronomy Department, University of California, 601 Campbell Hall, Berkeley, CA 94720, USA



**Abstract:**
I review multiwavelength observations of material seen around different types of evolved massive stars (i.e. red supergiants, yellow hypergiants, luminous blue variables, B[e] supergiants, and Wolf-Rayet stars), concentrating on diagnostics of mass, composition, and kinetic energy in both local and distant examples. Circumstellar material has significant implications for the evolutionary state of the star, the role of episodic mass loss in stellar evolution, and the roles of binarity and rotation in shaping the ejecta. This mass loss determines the type of supernova that results via the stripping of the star's outer layers, but the circumstellar gas can also profoundly influence the immediate pre-supernova environment. Dense circumstellar material can actually change the type of supernova that is seen when it is illuminated by the supernova or heated by the blast wave. As such, unresolved circumstellar material illuminated by distant supernovae can provide a way to study mass loss in massive stars in distant environments.

## 1 Introduction and Scope

There is a great variety of circumstellar material around massive stars. In the interest of brevity, I will restrict myself to discussing stars with detectable circumstellar *nebulae*, as distinguished from steady stellar *winds* or *disks* where the primary observable signature is seen in the spectrum and generally arises within several stellar radii (this was discussed in detail during the first session of this conference; see reviews by Owocki and Martins). By virtue of their high luminosity and radiation-driven winds, all massive stars shed mass in stellar winds, except perhaps at near zero metallicity. However, not all stars are surrounded by detectable circumstellar nebulae.

Furthermore, I will discuss only *circumstellar* material and not *interstellar* material (i.e. H II regions, photodissociation regions, giant molecular clouds; e.g., Zinnecker, these proceedings). Similarly, I will not delve into circumstellar accretion disks and outflows associated with the earliest formation phases of massive stars, as these were also discussed earlier in this conference (Beuther; these proceedings), nor will I discuss the phenomena of pulsar winds or black hole accretion disks. The main focus here is the circumstellar matter that results from the mass loss from massive stars in the course of their evolution up to core collapse.

It is surprisingly difficult to directly detect circumstellar gas and dust around extremely luminous central stars, and in part of this contribution I will review some of the tricks observers use to see circumstellar material in spite of the bright photospheric continuum light. In general, circumstellar nebulae can only be detected if the material is extremely dense and located relatively far from the

glare of the star. This requires densities several orders of magnitude higher than the densities of stellar winds at the same radius. Such high densities, in turn, imply that the nebulae are created by large amounts of matter ejected by the star. That is the chief reason they are of interest; namely, circumstellar nebulae provide a fossil record of the most important mass-loss phases experienced by stars.

Mass loss plays a critical role in the evolution of massive stars (e.g., Chiosi & Maeder 1986; Maeder & Meynet 2000; Meynet, these proceedings), and profoundly impacts the eventual supernova explosion (e.g., Woosley et al. 1993). Whether the mass loss that leads to Wolf-Rayet stars and stripped envelope supernovae (i.e. Types Ib and Ic) is due to steady winds, eruptions, or binary Roche lobe overflow (RLOF), and at exactly what initial masses this occurs, is still debated. In a recent paper, I have reviewed the connection between mass loss of progenitor stars and the types of observed supernovae more extensively (Smith et al. 2010).

Most importantly, the observational determination of the physical parameters of circumstellar nebulae — mass, composition, expansion age and kinetic energy, as well as global geometry and detailed structure — provide critical constraints for some of the most prodigious mass-loss phases of massive stars. This is particularly instructive for illuminating cases when the mass loss was strongly enhanced for a short time, and is therefore rarely observed directly (such as in brief giant LBV eruptions), or when the duration (and hence the cumulative mass-loss budget) is not well known. The chemical abundances of this ejected material tell us about the recent evolutionary phases of the star.

# 2 Types of Stars with Circumstellar Nebulae

As noted above, in order for a circumstellar nebula to be detectable, it must be very dense, with densities far exceeding those of normal stellar winds. Extremely high densities at large radii from the star can be achieved in two basic ways: (1) A dense shell can result from a sudden eruption or explosion that ejects a large amount of material from the star. This may happen, for example in an LBV eruption or in a red supergiant pulsation. The ejection of extremely dense shells may be accompanied by strong cooling to make dense clumps, or even dust grain formation, both of which may enhance the ability to be detected. (2) A dense shell nebula can result at the interface when a faster wind sweeps into a slow dense wind. In either case, the presence of a nebula requires a substantial change in the mass-loss behavior of the star on a relatively short timescale. For this reason, nebulae tend to be associated with stars in late transitional phases of evolution off the main sequence or immediately before a supernova. We do not generally see circumstellar nebulae around main sequence stars.[1] Some of the key types of stars that are normally associated with substantial circumstellar nebulae are outlined below, proceeding from cool to hot temperatures. I will try to highlight a demonstrative example of each.

## 2.1 Red Supergiants

Red supergiants have slow, dense, dusty winds. How the winds are driven from the stars is not completely understood, but it is likely that a combination of pulsations and radiation force on dust grains is at work, although there is also evidence for strongly enhanced episodes of mass loss as in the case of extreme red supergiants like VY CMa (Smith et al. 2001; 2009). Circumstellar material can sometimes be seen around red supergiants, but most notably in very nearby or very extreme cases.

[1]Incidentally, the fact that observable signatures of dense circumstellar material are absent around main-sequence O-type stars indicates that these stars quickly clear away all natal disk material associated with the star formation process.

The detectability of circumstellar material is enhanced by the fact tht the winds are slow and clumpy, giving rise to high density regions.

Betelgeuse is an extremely nearby example of a relatively normal red supergiant, but even at such close distances of only 150–200 pc (Harper et al. 2008), its circumstellar material is difficult to detect because its stellar wind mass-loss rate is only about $10^{-6}$ $M_{\odot}$ yr$^{-1}$ (Harper et al. 2008; Smith et al. 2009). Emission from its dusty wind has been resolved with mid-IR nulling interferometry (Hinz et al. 1998), and its circumstellar shell has been spatially resolved in emission lines like K I (Plez & Lambert 1994, 2002) and infrared CO bandhead emission (Smith et al. 2009).

VY CMa is a much more striking case, where the recent mass-loss rate is about $10^3$ times stronger than Betelgeuse, and is thought to be due to an enhanced mass-loss episode in the last 1,000 yr (Smith et al. 2001, 2009). This results in a dramatic circumstellar reflection nebula that is easily detected in visual-wavelength images with *HST* (Smith et al. 2001), polarized light (Jones et al. 2007), IR continuum emission from dust (Monnier et al. 1998), and in various spectral lines like K I (Smith 2004), infrared CO bandhead emission (Smith et al. 2009), and rotational lines of CO (Decin et al. 2006). Smith et al. (2009) have noted the stark difference between Betelgeuse and VY CMa, using the same techniques to observe circumstellar material around both stars.

## 2.2 Yellow Hypergiants

Like red supergiants, the yellow hypergiants (YHGs) have slow and dense, dusty winds which can give rise to detectable nebulae. These cases are rare, however, and most YHGs do not have easily detectable circumstellar nebulae. One dramatic example of a YHG with an observable nebula is IRC+10420 (see Oudmaijer 1998, Oudmaijer e al. 1996; Humphreys et al. 1997, 2002; Davies et al. 2007), which seems to be cruising across the top of the HR diagram, transitioning from a spectral type of late F to early A in just a few decades. If a YHG is seen to have a spatially resolved nebula, it is thought to result because the YHG is in a post-RSG phase. In the case of IRC+10420 this may be following a phase of enhanced RSG mass loss like VY CMa. Otherwise it would be quite difficult to explain the presence of OH masers (e.g., Bowers 1984) around such a warm star. These nebulae are dusty, seen in scattered starlight or thermal-IR emission, as well as in molecular transitions at longer wavelengths (Tiffany et al. 2010; Castro-Carrizio et al. 2001, 2007).

## 2.3 Luminous Blue Variables

LBVs are perhaps the best known examples of circumstellar nebulae around massive stars, exemplified in memorable *HST* images like those of $\eta$ Carinae (Morse et al. 1998) and the Pistol star (Figer et al. 1999). They are reminiscent of planetary nebulae in their complex structure and geometry, although LBV nebulae can be much more massive (see contributions by Vamratira-Nikov et al., Weis, Clark et al., and Wachter in these proceedings). Smith & Owocki (2006) noted several cases of luminous LBVs with nebulae of 10–20 $M_{\odot}$. These extremely massive shells – ejected relatively recently (typical ages of roughly $10^4$ yr or less) – indicate an extremely violent history of mass ejection, when these stars can potentially shed a large fraction of their initial mass in a disruptive event that lasts only a few years. This eruptive mass loss endures as one of the chief mysteries of stellar astrophysics, despite its importance in determining the fate of massive stars. Not all LBV nebulae are so massive, of course. Many are only of order 0.1 $M_{\odot}$. This is sometimes even seen in the same star: after ejecting $\sim$15 $M_{\odot}$ in its 1840s eruption, $\eta$ Carinae subsequently ejected 0.1–0.2 $M_{\odot}$ in its smaller 1890 eruption (Smith 2005).

The chemical abundances of LBV nebulae are generally nitrogen rich, indicating that nuclear material processed through the CNO cycle has risen to the surface of the star and has been ejected,

therefore indicating that these stars are in an advanced phase of their evolution (Davidson et al. 1986; Lamers et al. 2001; Smith & Morse 2004). In the case of $\eta$ Car, this N enhancement is very recent, occurring in jut the past few thousand years (Smith & Morse 2004; Smith et al. 2005).

The geometries of LBV nebulae are also interesting. LBV shells are often — although not always — bipolar. An obvious extreme example is $\eta$ Carinae, where the bipolar shape of the nebula seems consistent with expectations of mass loss from a rapidly rotating star (Smith 2006; Owocki 2003; Owocki et al. 1996; Dwarkadas & Owocki 2002; Smith & Townsend 2007). Bipolarity of LBV nebulae has often been attributed to various degrees of asymmetry in the pre-existing ambient material (e.g., Frank et al. 1995), although the origin of that pre-existing asymmetry does not have a clear explanation. Recent imaging of the nebula around the LBV HD 168625 (Smith 2007) showed a triple-ring structure almost identical to the nebula around SN 1987A (Burrows et al. 1995), providing a tantilizing link between LBVs and supernova progenitors (see below). On the other hand, some LBVs are only mildy ellipsoidal, like AG Car (see Weis, these proceedings), and some like P Cygni appear to be clearly spherical (Smith & Hartigan 2006). This suggests that we should avoid impulses to associate *all* LBV eruptions with stellar mergers or similar binary-induced effects.

## 2.4 B[e] supergiants and Equatorial Rings

The circumstellar material around B[e] stars was discussed in detail by Zickgraf et al. (1986, 1996; see posters at this meeting by Millour et al.; and Bonanos et al.). B[e] stars are thought to be surrounded by dusty equatorial tori with radii of order $10^3$ AU, making them bright IR sources, while gas in these slowly expanding tori give rise to their relatively narrow namesake forbidden emission lines. In many ways, the B[e] supergiants resemble less extreme versions of LBV nebulae. The spectral energy distributions of B[e] supergiants in the SMC and LMC look very similar to those of LBVs (Bonanos et al. 2009, 2010).

The origin of the equatorial circumstellar nebulae of B[e] stars remain unclear, but possibilities are that they arise from post-RSG evolution, equatorial mass loss from a recent RLOF phase, or that they arise from rapidly rotating stars. More detailed studies of B[e] stars and their circumstellar matter are certainly justified.

The dusty tori around B[e] supergiants with radii of $\sim 10^3$ AU may be related to an emerging class of early B supergiants with spatially resolved equatorial rings (see Smith et al. 2007; Smith 2007), including the progenitor of SN 1987A, SBW1 in the Carina Nebula, Sher 25 in NGC 3603, and HD 168625. Perhaps these equatorial rings are the expanding fossil remains of the B[e] tori (Smith et al. 2007).

## 2.5 Interacting Binaries

Although B[e] stars and LBVs are sometimes suspected to be binaries (and are indeed sometimes known to be binaries where the role of the companion star is unclear), there are also more clear-cut cases of binary-induced mass loss. Namely, there are very close interacting binaries that are sometimes even seen as eclipsing binaries, where we can see that they are in (or have recently been in) a RLOF phase of evolution.

One of the most interesting cases to mention is the massive, eclipsing, over-contact binary RY Scuti. To my knowledge, it is so far the only massive binary caught in the brief RLOF phase that also has a spatially resolved circumstellar nebula. This is interesting, because the nebula is not only torroidal (like those around B[e] supergiants), but also exhibits a bizarre double-ring structure (Smith et al. 2002; Gehrz et al. 2001). The properties of the nebula were discussed by Smith et al. (2002), while spectroscopy of the central binary system has been discussed recently by Grundstrom et al.

(2007). RY Scuti is extremely interesting, since the originally more massive member is thought to be caught in a brief transition to a WR star. This system therefore provides the rare opportunity to actually watch the stripping of the H envelope and the origin of a Type Ibc supernova progenitor in a binary system (e.g., Paczynski 1967). Smith et al. (2010) have concluded that this channel probably dominates the production of Type Ibc supernovae.

### 2.6 Wolf-Rayet Stars

Although Wolf-Rayet (WR) stars are famous for their strong winds, they also sometimes exhibit circumstellar nebulae, which come in two main flavors. One is the large wind-blown bubble nebulae that are generally seen around younger WN stars (see Stock & Barlow 2010). A famous example is NGC 6888. The raw material for these nebulae probably is not from the WR wind itself, however. Rather, the dense nebular gas is probably slower material ejected in a previous LBV or RSG phase, which is then swept into a dense bubble or shell by the faster WR wind.

A very different type of circumstellar nebula seen around WR stars is the dusty nebulae associated with WC+O binaries, either appearing as so-called "pinwheel" nebulae in circularized systems like WR104, or as episodic puffs of asymmetric dust production in eccentric systems like WR140. Although the dusty nature of WC stars had been known since the early days of IR astronomy (Gehrz & Hackwell 1974), the spectacular structure of these WR nebulae was only revealed by special high-resolution aperture synthesis imaging at near-IR wavelengths pioneered on the Keck telescope (see Tuthill et al. 1999; Monnier et al. 1999, 2002). In these cases, the dense gas and dust – which is much denser than the material normally found in a WR star wind – arises as a result of the compression and cooling in the colliding-wind shock of the WC+O binary (see Williams et al. 1990, 2001). The formation of graphite grains is likely facilitated by the C-rich material in the WC wind.

## 3 Multiwavelength Diagnostics of Circumstellar Material

### 3.1 Visual Wavelengths

At visual wavelengths, the two chief ways to spatially resolve circumstellar material are with starlight scattered by dust, and with intrinsic emission lines in the nebula. Because the central stars are bright, simple optical continuum imaging is only successful in a few remarkable cases, like $\eta$ Carinae, VY CMa, IRC+10420, etc. (see above), where the dusty nebula is very dense and the central star is partly obscured by the circumstellar dust. In other cases, polarimetric imaging or coronagraphy can help to suppress the direct light from the central star.

A more effective method is to use narrow-band imaging, long-slit spectroscopy, or IFU spectroscopy to detect extended emission lines from the circumstellar nebula. Concentrating on a nebular emission line formed only in the nebula helps suppress the bright continuum radiation from the central star. The most common probe is [N II] $\lambda$6583, which arises in most circumstellar nebulae over a wide range in ionization level, and can be especilly bright in the N-enriched gas around evolved massive stars (Davidson et al. 1986; Lamers et al. 2001; Smith & Morse 2004). Forbidden lines like [N II] are usually better than H$\alpha$, since H$\alpha$ is often an extremely strong emission line in the central star's spectrum as well. When high-resolution long-slit spectra are employed, lines like [N II] permit one to measure the expansion speed of a circumstellar shell (e.g., L. Smith 1994).

A lesser-known technique that has proven extremely useful for detecting nebulae around cooler stars (where N is neutral and [N II] cannot be seen) is the red resonance lines of K I. Extended K I $\lambda$7699 emission has been studied in detail around Betelgeuse and VY CMa, for example (Bernat & Lambert 1976; Bernet et al. 1978; Plez & Lambert 1994, 2002; Smith 2004). With high-resolution

long-slit spectroscopy of K I $\lambda$7699, one can perform the same types of kinematic studies as with [N II] around hotter stars. For nebulae around very hot stars, higher ionization lines like [Fe III] can also be useful, as in the case of RY Scuti (e.g., Smith et al. 2002).

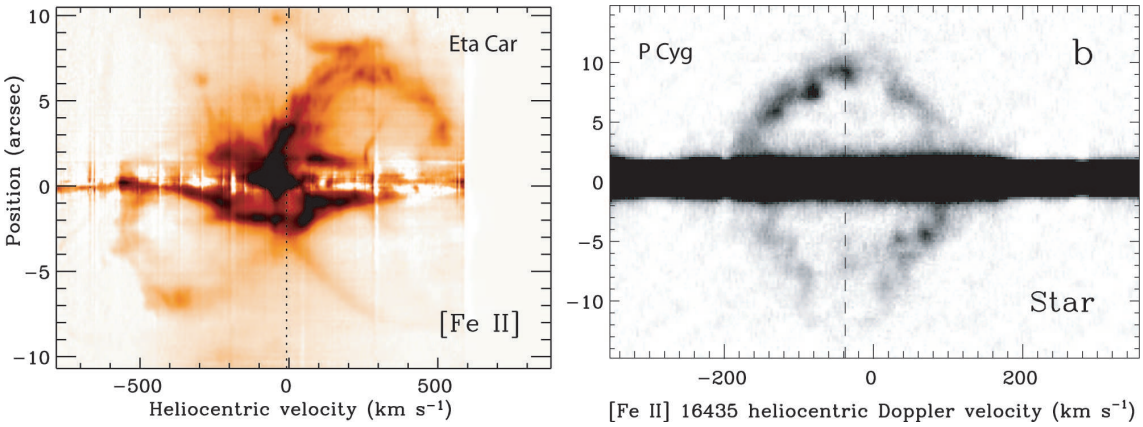


Figure 1: Long slit spectra of [Fe II] 1.644 $\mu$m around Eta Carinae (left; a) and P Cygni (right; b). The spectrum of Eta Car was taken with Phoenix on Gemini South (Smith 2006). The spectrum of P Cygni was taken with CSHELL on the IRTF (Smith & Hartigan 2006).

## 3.2 Near-IR

Near-IR wavelengths can provide a powerful probe of circumstellar material, especially in cases of massive stars that are obscured at visual wavelengths (in the Galactic Center, for example; Figer et al. 1999; Mauerhan et al. 2010). As with optical imaging, circumstellar shells can be resolved using scattered continuum starlight, although this is perhaps even more difficult than at visual wavelengths because of the lower scattering efficiency, unless the grains are large. However, with available technology, near-IR wavelengths have the advantage of adaptive-optics (AO) imaging or speckle-masking interferometry, as mentioned earlier. Again, polarimetric imaging and coronagraphy can help to suppress the bright central starlight.

Narrow-band imaging and long-slit spectroscopy are also used to resolve circumstellar material around massive stars in the near-IR, with H I lines such as Br $\gamma$ or (from space with *HST*) Pa$\alpha$ (e.g., Figer et al. 1999; Mauerhan et al. 2010). These lines are best around hotter stars where H is mostly ionized. In principle this is the same as H$\alpha$ imaging in the optical, but it can be used for obscured sources in the Galactic plane.

One of the most powerful but underused near-IR probes of circumstellar gas around massive stars involves spectroscopy or narrow-band imaging of infrared [Fe II] emission lines. In particular, [Fe II] $\lambda$16435 and $\lambda$12567 are two of the brightest lines in the near-IR spectra of LBVs and similar stars (Smith 2002), due to the relatively low excitation and high density of the gas. These two bright lines arise from the same upper energy level, and so their observed ratio can serve as a reliable measure of the reddening and extinction toward a source (see Smith & Hartigan 2006 for the atomic data and intrinsic line ratios). Flux ratios of some other adjacent [Fe II] lines to [Fe II] $\lambda$16435 serve as density diagnostics, while high-resolution spectra can provide the expansion speed of a shell. Detailed studies of $\eta$ Car and P Cygni have demonstrated the utility of these [Fe II] lines (Smith 2006; Smith & Hartigan 2006; see Figure 1).

Narrow-band imaging or spectroscopy of near-IR $H_2$ lines, like $H_2$ 1–0 S(1) at 2.122 $\mu$m, are also common tracers of shocked gas or dense gas irradiated by moderately strong non-ionizing radiation. However, these lines are rarely seen around hot stars because the $H_2$ is destroyed, and they are rarely

seen in cooler supergiants because they are not sufficiently excited. An unusual exception is the extremely bright $H_2$ lines in the Homunculus of $\eta$ Carinae (Smith 2006). In this source, the combination of a very young and dense nebula that is optically thick enough to be self-shielding allows the $H_2$ molecules to survive, while a surface layer of $H_2$ is struck by strong near-UV radiation from the luminous central star. As the Homunculus continues to expand and become more optically thin, the $H_2$ will be dissociated (see Smith & Ferland 2006 for details).

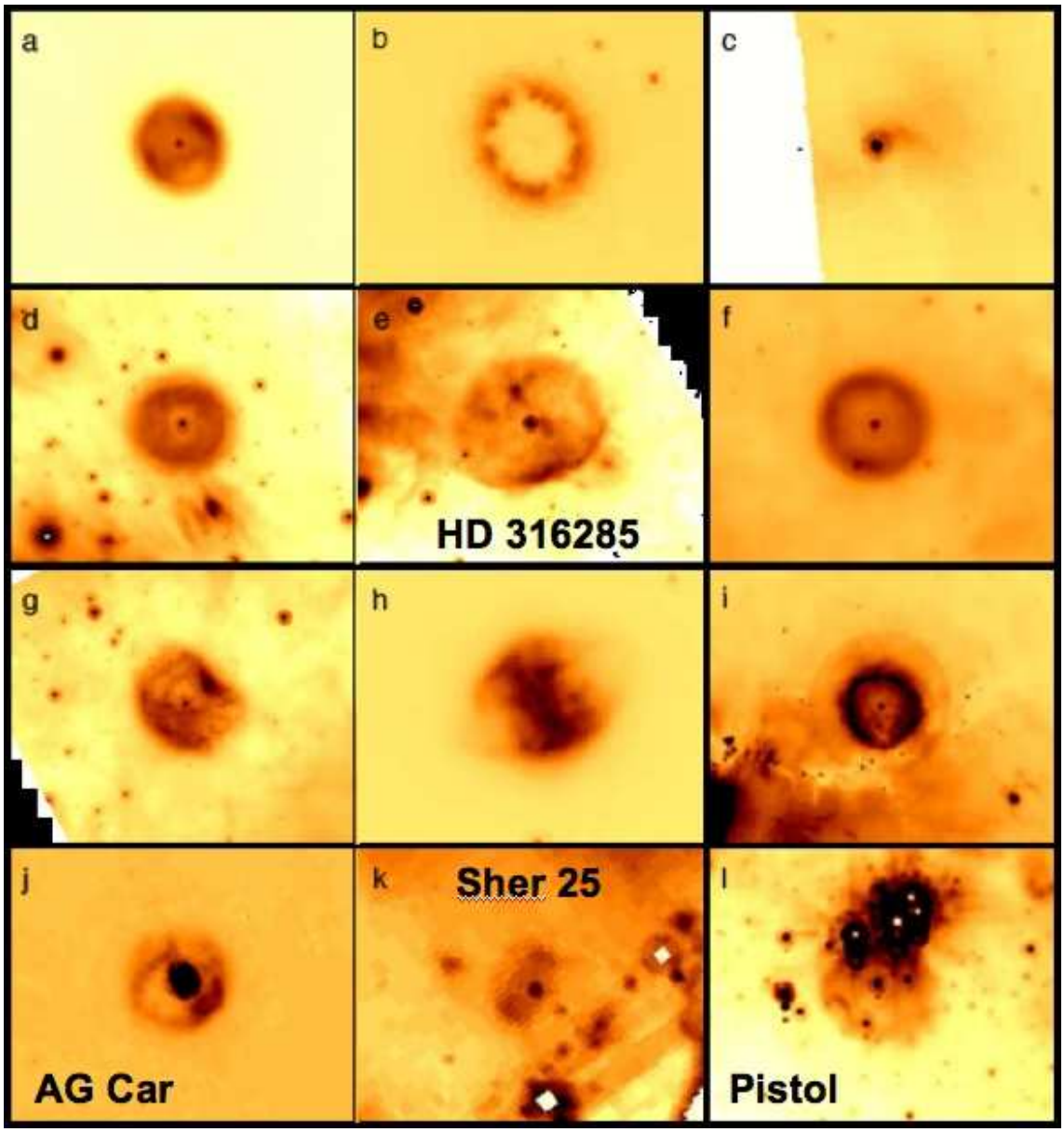


Figure 2: *Spitzer*/MIPS 24 $\mu$m images of shells around LBVs and related stars (adapted from Gvaramadze et al. 2010).

## 3.3 Mid-IR/Far-IR

Moving into the mid-IR and far-IR, circumstellar shells of massive stars become more easily observed because the glare of photospheric emission from the central stars is no longer a problem, and because thermal-IR radiation from warm dust grains is substantial. Extreme red supergiants like VY CMa and

NML Cygni have been favorite targets of ground-based mid-IR observers for decades because their circumstellar dust is bright and spatially extended, while $\eta$ Carinae is observed perpetually with every new mid-IR instrument that comes online in the southern hemisphere. Mid-IR observations played a special role in the history of our understanding of $\eta$ Carinae, providing our first clue that it is an extremely luminous but self-obscured star (Westphal & Neugebauer 1969). The young dust shell of $\eta$ Carinae acts as a calorimeter of the central star because it absorbs nearly all the star's UV radiation, and mid/far-IR observations provide our best estimates of the mass of the Homunculus (Smith et al. 2003).

Eta Carinae is an exceptional case, however, because its nebula is very young and very bright. For other LBVs, the shells are not so easy to detect in ground-based images because they are larger and more optically thin, and are therefore often too faint to detect in the mid-IR through the Earth's atmosphere. However, space-based IR telescopes have provided key information on a number of dusty shells around LBVs (e.g., Voors et al. 2000; Trams et al. 1998; Egan et al. 2002; Clark et al. 2003). In particular, recent surveys of the Galactic plane with the IRAC and MIPS instruments on *Spitzer* have revealed a large number of extended mid-IR shells around LBVs and related stars (see Fig. 2; Gvardmadze et al. 2010; Wachter et al. 2010; Smith 2007). This sample has the potential to tell us how much mass is typically ejected by an LBV, and to identify previously unrecognized LBVs and WR stars. We eagerly anticipate results on the far-IR emission from these shells with *Herchel*. Longer mid-IR and far-IR wavelengths are useful, because they have the potential to detect cooler dust in the shell, which may correspond to a large fraction of the total mass.

In addition to very extended shell nebulae, the more compact dusty pinwheels and episodic ejections associated with colliding-wind WC+O binaries are also spatially resolved in the thermal-IR, as noted earlier (Tuthill et al. 1999; Monnier et al. 1999, 2002), providing a powerful probe of a unique mass-loss phenomenon.

## 3.4 X-rays

The spatially resolved nebulae around massive stars are not often detected in X-rays, since strong shocks (and hence, strong differences in ejection velocity over a short period of time) are needed to produce sufficiently bright X-rays far from the star. The study of *diffuse* X-ray emission asociated with massive stars is mainly concentrated toward SNe and SN remnants (see below). A notable exception, again, is the peculiar case of $\eta$ Carinae, where a strong blast wave from the 19th century eruption is overtaking ejecta from a previous eruption (Smith 2008), giving rise to a spectacular soft X-ray shell made famous in *Chandra* images (e.g., Seward et al. 2001). The study of massive stars in X-rays is weighted heavily toward colliding wind binaries or unresolved soft X-ray emission from the winds of O-type stars.

## 3.5 Radio

At radio wavelengths, continuum free-free radiation traces the same photoionized gas around hot massive stars that can be observed with H$\alpha$ emission, but without such strong continuum radiation from the central star, and free from line-of-sight extinction. This is particularly useful for studying the nebulae of hotter LBVs and WR stars (e.g., Duncan & White 2002).

Radio wavelengths also provide unique probes of molecular shells around massive stars, most commonly seen around cooler supergiants. In particular, molecular masers like SiO, $H_2O$, and OH can be observed at very high spatial resolution with radio interferometers, and have yielded unique and valuable information about the structure and expansion of shells around evolved cool stars (e.g., Bowers et al. 1993; Benson & Mutel 1979, 1982; Marvel 1997; Boboltz & Marvel 2000; Trigilio et

al. 1998). One can actually follow the proper motion and Doppler velocity of individual maser spots, tracing out the structure, expansion, and rotation of the inner winds of these stars. Molecular shells are not generally observed around hot stars because they are quickly dissociated by UV radiation. However, they are seen in some cases of young WR stars or YHGs that are in a post-RSG phase, as noted earlier for IRC+10420. The N-enriched shells of LBVs may be detectable in ammonia, which has been detected in $\eta$ Car (Smith et al. 2006), but has not been searched for extensively in other sources.

# 4 Supernova Blast Waves Crashing into Pre-Supernova Circumstellar Material

When a supernova (SN) explodes, it sends a flash of UV radiation and a strong blast wave out into the surrounding medium. In this way, SNe illuminate the circumstellar material that was ejected by the star *before* the SN. As the shock expands it can interact with either circumstellar or interstellar material, giving rise to a SN remnant. The posterchild for a SN remnant interacting with dense circumstellar material ejected by its progenitor is Cas A (e.g., Chevalier & Oishi 2003). Slow-moving N-rich "flocculi" (Fesen & Becker 1991; Chevalier & Kirshner 1978) indicate that the overtaken material was circumstellar rather than interstellar, and that the progenitor was at least a moderately massive evolved star with a fairly slow wind (Chevalier & Oishi 2003).

Perhaps the most famous case of a SN blast wave interacting with circumstellar material is SN 1987A. Almost immediately, the UV flash of the SN shock breakout photoionized the triple ring nebula seen in *HST* images (Burrows et al. 1995). After about 10 years, the SN blast wave began crashing into the equatorial ring seen in these images, and this collision is still unfolding (Michael et al. 2000; Sonneborn et al. 1997; Sugerman et al. 2002). The complex shock interaction is the focus of an ongoing multiwavelength campaign, and provides an enormous reservoir of information about shock physics as well as pre-SN mass loss of the progenitor star. Since the blue progenitor contradicted expectations of stellar evolution models, it has been suggested that the progenitor star underwent a binary merger event to produce the triple-ring nebula (e.g., Morris & Podsiadlowski 2007), but comparisons to LBV nebulae have also been made (Smith 2007).

Sometimes the interaction between the SN shock and circumstellar gas happens much sooner and is even more dramatic. In the case of Type IIn, this shock interaction with the nearest circumstellar gas can happen immediately, completely altering the apparent spectrum of the SN and in some cases markedly increasing the luminosity of the SN. The name "IIn" comes from the narrow H emission lines in the spectrum, arising from the slow shocked CSM gas. The dense circumstellar material decelerates the blast wave and thermalizes its kinetic energy. In some cases this thermal energy is radiated as visual light before adiabatic expansion can cool the gas, thus producing some of the most luminous SNe in the universe with $\sim 10^{51}$ ergs radiated in visual light alone (e.g., Smith & McCray 2007, Smith et al. 2007, 2010; Woosley et al. 2007; van Marle et al. 2010; see Figure 3). By studying the time evolution of the luminosity and spectral properties of SNe IIn in the year or two after discovery, we can deduce the density and velocity of circumstellar matter at each radial position overtaken by the shock. An exemplary case concerns the spectral evolution and light echo of SN 2006gy, from which a circumstellar medium closely resembling that of $\eta$ Carinae has been deduced (Smith et al. 2010). We can therefore reconstruct the mass-loss rate and kinetic energy of pre-SN mass ejections as a function of time immediately before the SN explosion occurred. Aside from being lucky enough to be watching when an exceptional Galactic SN occurs, this is our most powerful tool for studying how massive stars behave in the rapid nuclear timescales immediately before they suffer core collapse.

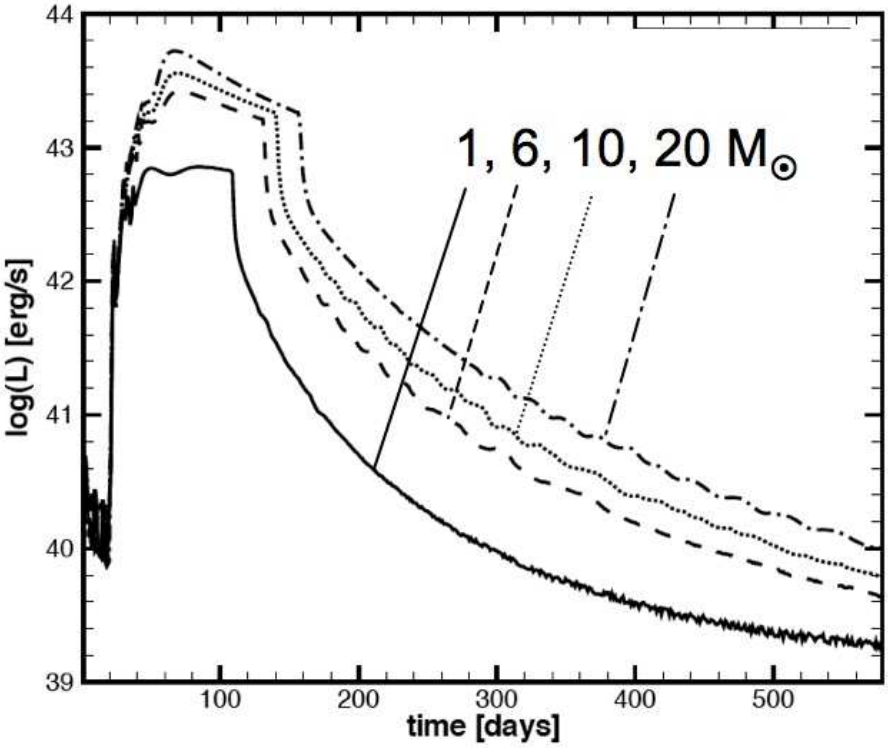


Figure 3: Theoretical light curves of a normal SN shock crashing into dense circumstellar gas with a range of masses from 1–20 $M_{\odot}$ (from van Marle et al. 2010). A normal Type II-P supernova has a peak luminosity of about $10^{42}$ erg $s^{-1}$.

The potential of using SNe IIn to learn about circumstellar structure and pre-SN evolution is extremely exciting. Not only does this shock interaction produce some of the most luminous SNe known, potentialy observable at high redshift, but it also can provide diagnostics of the detailed properties of circumstellar gas around a single (or binary) star at distances far beyond where we could ever hope to spatially resolve a circumstellar nebula.

# Acknowledgements

I thank the conference organizers for covering part of my travel expenses at the conference.

# References

Benson, J.M., & Mutel, R.L. 1979, ApJ, 233, 119
Benson, J.M., & Mutel, R.L. 1982, ApJ, 253, 199
Bernet, A.P., & Lambert, D.L. 1976, ApJ, 210, 395
Bernet, A.P., et al. 1978, ApJ, 219, 532
Boboltz, D.A., & Marvel, K.B. 2000, ApJ, 545, L149
Bonanos, A., et al. 2009, AJ, 138, 1003
Bonanos, A., et al. 2010, AJ, 140, 416
Bowers, P.F. 1984, 279, 350
Bowers, P.F., Claussen, M.J., & Johnston, K.J. 1993, AJ, 104, 284
Burrows, C.J., et al. 1995, ApJ, 452, 680
Castro-Carrizo, A., Lucas, R., Bujarrabal, V., Colomer, F., & Alcolea, J. 2001, A&A, 368, L34

Castro-Carrizo, A., Quintana-Lacaci, G., Bujarrabal, V., Neri, R., & Alcolea, J. 2007, A&A, 465, 457
Chevalier, R.A., & Kirshner, R.P. 1978, ApJ, 219, 931
Chevalier, R.A., & Oishi, J. 2003, ApJ, 593, L23
Chiosi, C., & Maeder, A. 1986, ARAA, 24, 329
Clark, J.S., Egan, M., Crowther, P., et al. 2003, A&A, 412, 185
Davidson, K., Dufour, R., Walborn, N.R., & Gull, T.R. 1986, ApJ, 305, 867
Davies, B., Oudmaijer, R.D., & Sahu, K.C. 2007, ApJ, 671, 2059
Decin, L., et al. 2006, A&A, 456, 549
Duncan, R.A., & White, S.M. 2002, MNRAS, 330, 63
Dwarkadas, V.V., & Owocki, S.P. 2002, ApJ, 581, 1337
Egan, M., Clark, J.S., Mizuno, D.R., et al. 2002ApJ, 572, 288
Fesen, R.A., & Becker, R.H. 1991, ApJ, 371, 621
Figer, D., McClean, I.S., & Morris, M. 1999, ApJ, 514, 202
Frank, A., Balick, B., & Davidson, K. 1995, ApJ, 441, L77
Gehrz, R.D., & Hackwell, J.A. 1974, ApJ, 194, 619
Gehrz, R.D., Smith, N., & Jones, B., et al. 2001, ApJ, 559, 395
Grundstrom, E., et al. 2007, ApJ, 667, 505
Gvaramadze, V., et al. 2010, MNRAS, 405, 1047
Harper, G., Brown, A., & Guinan, E. 2008, AJ, 135, 1430
Hinz, P.M., et al. 1998, Nature, 395, 251
Humphreys, R.M., Smith, N., Davidson, K., et al. 1997, AJ, 114, 2778
Humphreys, R.M., Davidson, K., & Smith, N. 2002, AJ, 124, 1026
Jones, T.J., et al. 2007, AJ, 133, 2730
Lamers, H.J.G.L.M., et al. 2001, ApJ, 551, 764
Maeder, A., & Meynet, G. 2000, A&A, 361, 159
Marvel, K.B. 1997, PASP, 104, 1286
Mauerhan, J., et al. 2010, arXiv:1009.2769
Michael, E., et al. 2000, ApJ, 542, L53
Monnier, J.D., Geballe, T.R., & Danchi, W.C. 1998, ApJ, 502, 833
Monnier, J.D., Tuthill, P., & Danchi, W.C. 1999, ApJ, 525, L97
Monnier, J.D., Tuthill, P., & Danchi, W.C. 2002, ApJ, 567, L137
Morris, T., & Podsiadlowski, P. 2007, Science, 351, 1130
Morse, J.A., et al. 1998, AJ, 116, 2443
Oudmaijer, R.D. 1996, A&AS, 129, 541
Oudmaijer, R.D., Groenewegen, M.A.T., Matthews, H.E., Blommaert, J.A.D.L., & Sahu, K.C. 1996, MNRAS, 280, 1062
Owocki, S.P. 2003, in IAU Symp. 212, 281
Owocki, S.P., Cranmer, S.R., & Gayley, K.G. 1996, ApJ, 472, L115
Plez, B., & Lambert, D.L. 1994, ApJ, 425, L101
Plez, B., & Lambert, D.L. 2002, A&A,386, 1009
Paczynski, B. 1967, Acta Astron., 17, 355
Seward, F., et al. 2001, ApJ, 553, 832
Smith, L. 1994, ApSS, 216, 291
Smith, N. 2002, MNRAS, 336, L22
Smith, N. 2004, MNRAS, 349, L31
Smith, N. 2005, MNRAS, 357, 1330
Smith, N. 2006, ApJ, 644, 1151
Smith, N. 2007, AJ, 133, 1034
Smith, N. 2008, Nature, 455, 201
Smith, N., & Ferland, G.R. 2007, ApJ, 655, 911
Smith, N., & Hartigan, P. 2006, ApJ, 638, 1045
Smith, N., & McCray, R. 2007
Smith, N., & Morse, J.A. 2004, ApJ, 605, 854
Smith, N., & Owocki, S.P. 2006, ApJ, 645, L45
Smith, N., & Townsend, R.H.D. 2007, ApJ, 666, 967
Smith, N., et al. 2001, AJ, 121, 1111
Smith, N., Gehrz, R.D., Hinz, P.M., et al. 2003, AJ, 125, 1458
Smith, N., et al. 2002, ApJ, 578, 464

Smith, N., Brooks, K.J., Koribalski, B.S., & Bally, J. 2006, ApJ, 645, L41
Smith, N., Morse, J.A., & Bally, J. 2005, AJ, 130, 1778
Smith, N., Bally, J., & Walawender, J. 2007, AJ, 134, 846
Smith, N., Hinkle, K.H., & Ryde, N. 2009, AJ, 137, 3558
Smith, N., et al. 2010, ApJ, 709, 856
Smith, N., et al. 2010, MNRAS, in press; arXiv:1006.3899
Sonneborn, G., et al. 1998, ApJ, 492, L139
Stahl, O. 1987, A&A, 182, 229
Sugerman, B.E.K. 2000, ApJ, 572, 209
Tiffany, C., Humphreys, R.M., Jones, T.J., & Davidson, K. 2010, AJ, 140, 339
Trams, N.R., et al. 1998, Ap&SS, 255, 195
Trigilio, C., Umana, G., & Cohen, R.J. 1998, MNRAS, 297, 497
Tuthill, P.C., Monnier, J.D., & Danchi, W.C. 1999, Nature, 398, 486
Voors, R.H.M., et al. 2000, A&A, 356, 501
Wachter, S., et al. 2010, AJ, 139, 2330
Westphal, J.A., & Neugebauer, G. 1969, ApJ, 156, L45
Williams, P.M., et al. 1990, MNRAS, 243, 662
Williams, P.M., et al. 2001, MNRAS, 324, 156
Woosley, S.E., Langer, N., & Weaver, T.A. 1993, ApJ, 411, 823
Zickgraf, F.J., et al. 1986, A&A, 163, 119
Zickgraf, F.J., et al. 1996, A&A, 309, 505